

Stable and Metastable Phases in the Systems $\text{AgI-Ag}_2\text{XO}_4$ ($\text{X}=\text{Cr, Mo, W}$)

Aldo Magistris, Gaetano Chiodelli, and Giuseppina Viganò Campari

Centro di studio per la termodinamica ed elettrochimica dei sistemi salini fusi e solidi del CNR
c/o Istituto di Chimica Fisica e di Elettrochimica dell'Università di Pavia (Italy)

(Z. Naturforsch. 31a, 974–977 [1976]; received May 14, 1976)

DTA and powder x-ray diffraction measurements allowed to draw the phase diagrams of the systems $\text{AgI-Ag}_2\text{XO}_4$ ($\text{X}=\text{Cr, Mo, W}$).

A more detailed investigation was devoted to the composition range around $X_{\text{AgI}}=0.8$, where in preliminary tests it was observed that the room temperature ionic conductivity strongly depends on the thermal treatment of the sample.

By quenching mixtures at $X_{\text{AgI}}=0.8$, glass-like phases with high conductivity were obtained; in the systems $\text{AgI-Ag}_2\text{CrO}_4$ and $\text{AgI-Ag}_2\text{MoO}_4$ the subsequent crystallization gave rise to non conducting phases, whereas the occurrence of the highly conducting compound $4\text{AgI}\cdot\text{Ag}_2\text{WO}_4$ was recognized in the third system investigated.

Introduction

Many papers were recently devoted to investigations of solid electrolytes containing AgI which show high ionic conductivity at room temperature. Noteworthy results were obtained for the systems $\text{AgI-Ag}_n\text{XO}_4$ and $\text{AgI-Ag}_n\text{X}_2\text{O}_4$ ($\text{X} = \text{W, Cr, Mo, P, V, Te, Se, As}$)¹⁻⁶.

In a previous work by our group², electric a. c. conductivity and e. m. f. determinations were carried out on solid electrolytes formed with AgI and Ag_2XO_4 ($\text{X} = \text{Cr, Mo, W}$) of a composition close to 80 mole% AgI . These electrolytes, prepared by quenching of the corresponding molten mixtures, showed an electric conductivity at 23 °C as large as $10^{-2} \Omega^{-1}\text{cm}^{-1}$. In preliminary tests, transport number determinations (Tubandt's method) allowed to establish that the silver ions are the only carriers in these materials.

Furthermore it was observed that, after annealing at $T > 80^\circ\text{C}$, the original materials, excepted the case of the $\text{AgI-Ag}_2\text{WO}_4$ system, showed a much lower conductivity at room temperature (Figure 1).

In order to attain a more detailed information about such high conducting phases, in the present work the phase diagrams of these systems were defined through DTA and x-ray diffraction determinations on samples subjected to different thermal treatments.

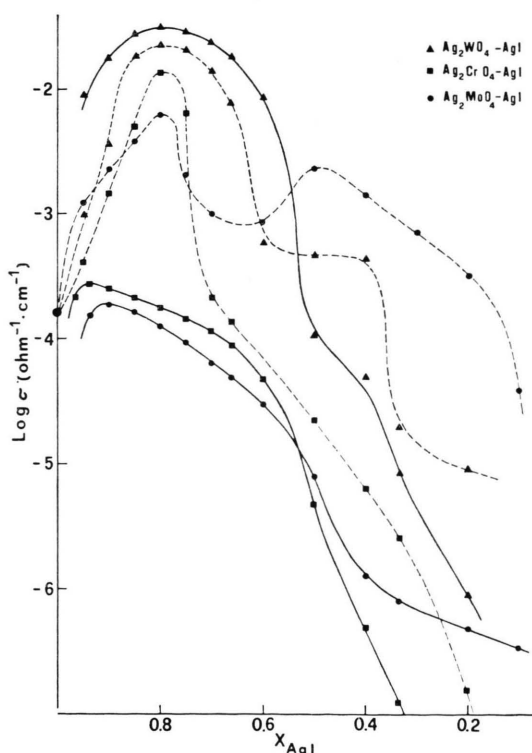


Fig. 1. Electrical conductivity at 23 °C vs. composition in the systems $\text{AgI-Ag}_2\text{XO}_4$ ($\text{X} = \text{Cr, Mo, W}$). Data concern quenched (dashed lines) and annealed (full lines) samples; the arrangement of the conductivity cells and the instrumental apparatus are reported in a previous work².

Experimental

Fluka puriss. AgI and Ag_2CrO_4 were directly employed, whereas Ag_2MoO_4 and Ag_2WO_4 were precipitated from aqueous C. Erba RP AgNO_3 with C.

Reprint requests to Aldo Magistris, Istituto di Chimica Fisica e di Elettrochimica della Università di Pavia, Viale Taramelli, I-27100 Pavia (Italy).



Dieses Werk wurde im Jahr 2013 vom Verlag Zeitschrift für Naturforschung in Zusammenarbeit mit der Max-Planck-Gesellschaft zur Förderung der Wissenschaften e.V. digitalisiert und unter folgender Lizenz veröffentlicht: Creative Commons Namensnennung-Keine Bearbeitung 3.0 Deutschland Lizenz.

Zum 01.01.2015 ist eine Anpassung der Lizenzbedingungen (Entfall der Creative Commons Lizenzbedingung „Keine Bearbeitung“) beabsichtigt, um eine Nachnutzung auch im Rahmen zukünftiger wissenschaftlicher Nutzungsformen zu ermöglichen.

This work has been digitalized and published in 2013 by Verlag Zeitschrift für Naturforschung in cooperation with the Max Planck Society for the Advancement of Science under a Creative Commons Attribution-NoDerivs 3.0 Germany License.

On 01.01.2015 it is planned to change the License Conditions (the removal of the Creative Commons License condition “no derivative works”). This is to allow reuse in the area of future scientific usage.

Erba RP Na₂MoO₄ or BDH Analar Na₂WO₄ and then thoroughly washed and dried at 120 °C under vacuum and protected from light.

Salt mixtures with different compositions were heated in a sealed quartz tube at 100 °C above the melting point, then quenched in liquid N₂ and grinded.

For DTA determinations a Du Pont "900 DSC" was employed; 100 mg powder samples were sealed in silver caps; carborundum was used as reference; the heating rate generally was 10 deg·min⁻¹.

X-ray diffraction patterns of powdered salts were obtained at room temperature with the Cu K α radiation in the Philips camera PW 1011/00 working at 18 mA and 40 kV.

Results and Discussion

DTA and x-ray results concern samples which had been subjected to either quenching from 100 °C above the melting point (i. e. in the same conditions which gave high conducting materials²) or an-

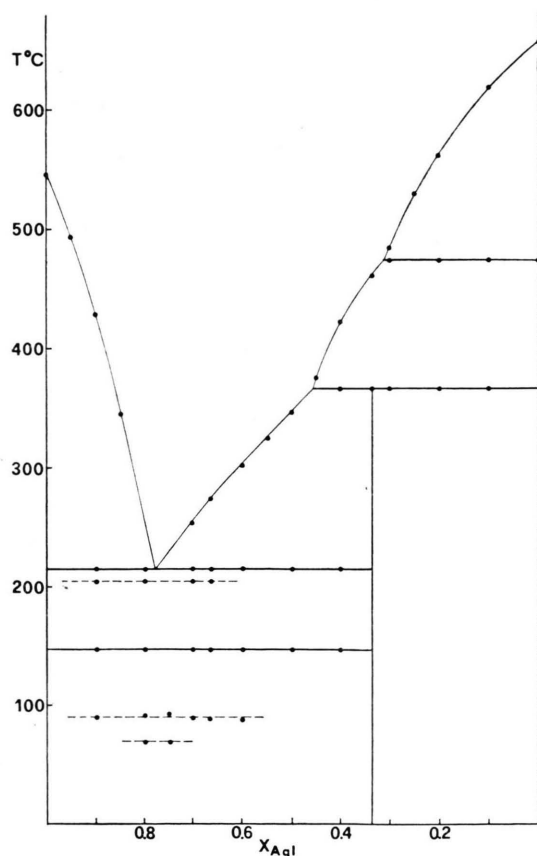


Fig. 2 a. Phase diagram of the system AgI—Ag₂CrO₄.

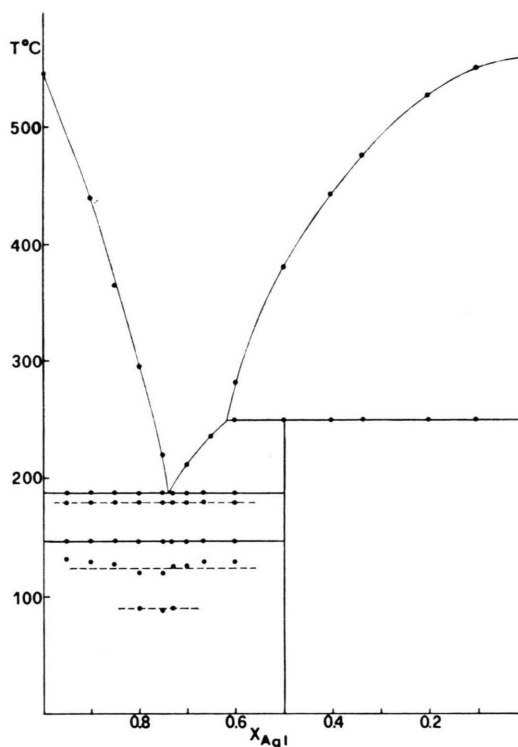


Fig. 2 b. Phase diagram of the system AgI—Ag₂MoO₄.

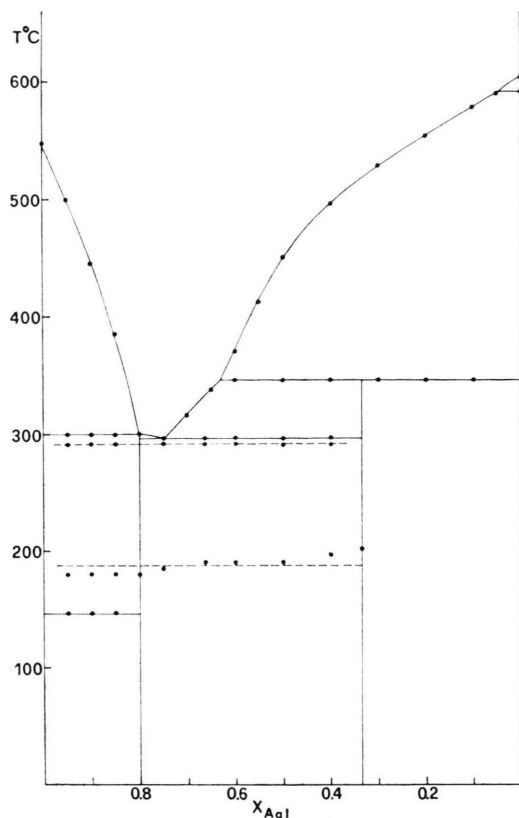
nealing one week at 20 °C below the eutectic temperature.

The phase diagrams of the three systems studied are shown in Fig. 2 a, 2 b, and 2 c, where the dashed and full lines refer to the quenched and annealed samples respectively.

As for the annealed samples, the following results were obtained.

System AgI—Ag₂CrO₄ (Fig. 2 a): a eutectic at $X_{\text{AgI}} = 0.78$, $T = 215$ °C and an incongruent compound AgI·2Ag₂CrO₄ decomposing at 367 °C; Ag₂CrO₄ (m.p. 657 °C) shows a phase transition at 474 °C. System AgI—Ag₂MoO₄ (Fig. 2 b): a eutectic at $X_{\text{AgI}} = 0.74$, $T = 188$ °C and an incongruent compound AgI·Ag₂MoO₄ decomposing at 250 °C; Ag₂MoO₄ melts at 558 °C.

System AgI—Ag₂WO₄ (Fig. 2 c): a eutectic at $X_{\text{AgI}} = 0.75$, $T = 297$ °C and two incongruent compounds, 4AgI·Ag₂WO₄ and AgI·2Ag₂WO₄, which decompose at 308 and 364 °C respectively; Ag₂WO₄ (m.p. 604 °C) shows a phase transition near the melting point (592 °C). The data concerning this system are in agreement with the phase diagram by Takahashi¹.

Fig. 2 c. Phase diagram of the system $\text{AgI}-\text{Ag}_2\text{WO}_4$.

The occurrence of the mentioned intermediate compounds is supported by the x-ray diffraction patterns obtained from annealed samples and reported in Table 1.

DTA and x-ray diffraction data taken on quenched samples are remarkably different from those taken on the annealed ones, particularly in the case of the AgI rich compositions.

For a wide composition range around the eutectic points, the $\text{AgI}-\text{Ag}_2\text{CrO}_4$ and $\text{AgI}-\text{Ag}_2\text{MoO}_4$ quenched samples showed two exothermic effects: the first, quite diffuse at $70-90^\circ\text{C}$, the second, more evident at $100-120^\circ\text{C}$ (Figure 3 a). The latter attained the largest intensity at a composition close to $X_{\text{AgI}}=0.8$. Such effects are represented in the phase diagrams by dashed lines (Fig. 2 a and 2 b). No effect of this kind was detected in any annealed samples (Figure 3 b).

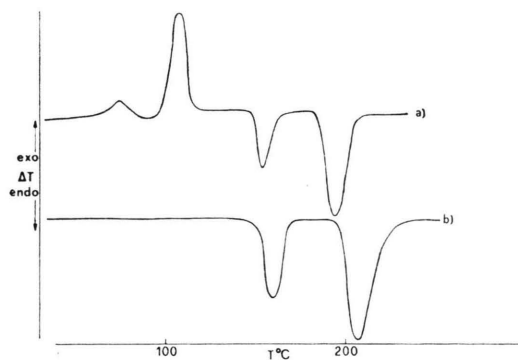
A detailed investigation was devoted to the study of the thermal effect related to the $\beta \rightarrow \alpha$ transition of AgI at 147°C . It was observed that in the systems containing Ag_2CrO_4 and Ag_2MoO_4 the

Table 1. Powder x-ray patterns for the systems $\text{AgI}-\text{Ag}_2\text{CrO}_4$, $\text{AgI}-\text{Ag}_2\text{MoO}_4$, and $\text{AgI}-\text{Ag}_2\text{WO}_4$ (only the most intensive signals are reported).

Ag_2CrO_4		$\text{AgI} \cdot 2 \text{Ag}_2\text{CrO}_4$		AgI	
$d(\text{\AA})$	I	$d(\text{\AA})$	I	$d(\text{\AA})$	I
2.87	100	5.18	25	3.75	100
2.85	90	2.78	70	2.30	70
2.77	50	2.74	100	1.96	40
2.05	20	2.42	40		
1.99	20	2.26	25		

Ag_2MoO_4		$\text{AgI} \cdot \text{Ag}_2\text{MoO}_4$			
$d(\text{\AA})$	I	$d(\text{\AA})$	I		
3.29	25	3.67	20		
2.81	100	3.18	100		
2.69	25	3.07	20		
2.33	20	3.01	20		
1.79	40				
1.65	40				

Ag_2WO_4		$4 \text{AgI} \cdot \text{Ag}_2\text{WO}_4$		$\text{AgI} \cdot 2 \text{Ag}_2\text{WO}_4$	
$d(\text{\AA})$	I	$d(\text{\AA})$	I	$d(\text{\AA})$	I
2.96	12	3.68	70	3.05	30
2.84	100	3.46	100	2.99	100
2.72	20	2.75	80	2.86	60
2.01	30	2.56	80	2.81	50

Fig. 3. Typical DTA patterns for samples with AgI rich composition: a) quenched, b) annealed.

amount of AgI undergoing the transition, which was estimated through a quantitative determination of the corresponding DTA peak area, which obviously is 100% for pure AgI , decreases according to the expected law for a diphasic mixture of AgI and the intermediate compound reported in the corresponding phase diagram, whereas for the quenched samples the DTA peak area is always smaller than for the annealed ones (Fig. 4 a and 4 b). As for the system $\text{AgI}-\text{Ag}_2\text{WO}_4$, the thermograms show no exothermic peaks before the AgI phase transition,

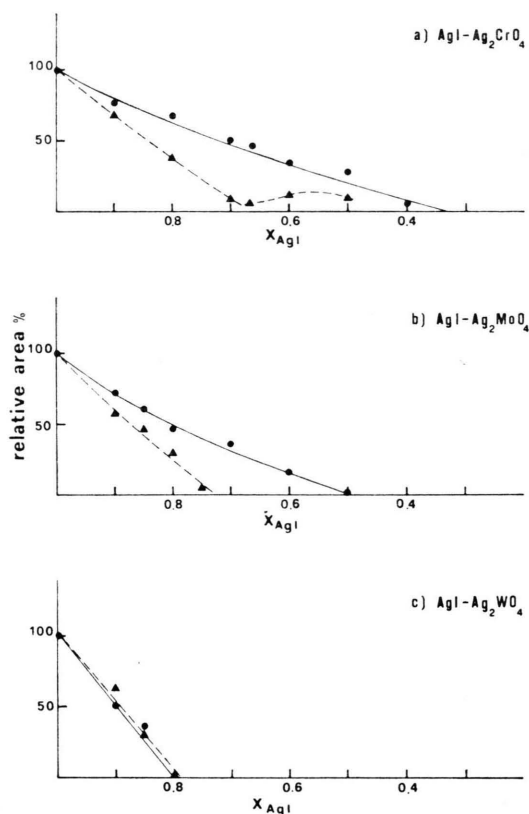


Fig. 4. Relative DTA peak areas of the $\beta \rightarrow \alpha$ AgI transition (147 °C) vs. composition in the systems: a) AgI–Ag₂CrO₄, b) AgI–Ag₂MoO₄, c) AgI–Ag₂WO₄.

while a single peak (exothermic) appears at about 190 °C. The area underlying the 147 °C peak for quenched samples is generally as large as for the annealed ones and vanishes for both kinds of treatment at $X_{\text{AgI}} = 0.8$ (Figure 4 c).

Another difference between quenched and annealed samples is an endothermic peak which can be observed only in the former ones just below (5–10 °C) the eutectic point.

The occurrence of the exothermic signals in the quenched samples thermograms (Fig. 3 a) might be compared with the typical thermograms obtained from amorphous materials⁷. Accordingly, the first thermal effect would correspond to the glass transi-

tion temperature, whereas the second exothermic peak would be due to crystallization.

Investigation by means of the microscope confirms this hypothesis particularly for the system AgI–Ag₂MoO₄, where apparent softening phenomena of the quenched materials, observed at about 80 °C, are followed by a crystallization process at higher temperature (≈ 120 °C).

A more direct support is obtained from the x-ray analysis carried out, at room temperature, on quenched samples. Indeed, the results concerning the range of the compositions richer in AgI were similar to those reported by Kunze for AgI–Ag₂SeO₄⁵. The patterns show only peaks due to γ -AgI, the intensities of which decrease with the AgI content and vanish at $X_{\text{AgI}} = 0.8$. For the composition $X_{\text{AgI}} = 0.8$ only a few diffuse bands are observed which might be interpreted as due to an amorphous substance. In the case of the system AgI–Ag₂WO₄ the observed patterns were quite complex. At $X_{\text{AgI}} = 0.8$ very weak signals were detected at the same position of more intense ones already attributed to the compound $4\text{AgI} \cdot \text{Ag}_2\text{WO}_4$ in the annealed samples; at $X_{\text{AgI}} = 0.66$ a few signals were also observed which cannot be reliably referred to any of the identified phases and might be attributed to the compound $2\text{AgI} \cdot \text{Ag}_2\text{WO}_4$ reported by Takahashi¹.

On the basis of the above results one may conclude that, at least for the systems AgI–Ag₂CrO₄ and AgI–Ag₂MoO₄, the quenched mixtures at $X_{\text{AgI}} = 0.8$ are substantially metastable amorphous phases; accordingly, the time dependent decrease of the conductivity observed at $T > 60$ °C⁴ might be due to a crystallization process which allows the formation of low conducting phases, i.e. AgI and AgI·Ag₂CrO₄ or AgI·Ag₂MoO₄. As for the system AgI–Ag₂WO₄, the general similarity between the behaviour of quenched and annealed samples at $X_{\text{AgI}} = 0.8$ might be explained assuming that the highly conducting compound $4\text{AgI} \cdot \text{Ag}_2\text{WO}_4$ is formed, the conductivity of which rises with rising temperature² and takes time independent values up to the melting point.

¹ T. Takahashi, S. Ikeda, and O. Yamamoto, J. Electrochem. Soc. **120**, 647 [1973].

² G. Chiodelli, A. Magistris, and A. Schiraldi, Electrochim. Acta **19**, 655 [1974].

³ T. Takahashi, S. Ikeda, and O. Yamamoto, J. Electrochem. Soc. **119**, 477 [1972].

⁴ A. Schiraldi, G. Chiodelli, and A. Magistris, J. Appl. Electrochem., 1976 in press.

⁵ B. Scrosati, F. Papaleo, G. Pistoia, and M. Lazzari, J. Electrochem. Soc. **122**, 339 [1975].

⁶ D. Kunze, "Fast Ion Transport in Solids", W. van Gool, Ed., North Holland, Amsterdam 1973, p. 405.

⁷ See e.g.: Wilbur and Dowson in "Differential Thermal Analysis", vol. II, Ed. Mackenzie, p. 237; D. D. Thornburg, Mat. Res. Bull. **9**, 1481 [1974].